HHS Public Access

Author manuscript

Chem Biol Drug Des. Author manuscript; available in PMC 2023 July 01.

Published in final edited form as:

Chem Biol Drug Des. 2022 July ; 100(1): 64–79. doi:10.1111/cbdd.14053.

Sulfonated non-saccharide molecules and human factor XIa: Enzyme inhibition and computational studies

Rami A. Al-Horani[1], **Elnaz Parsaeian**[1], **Mariam Mohammad**[1], **Madhusoodanan Mottamal**[2]

[1]Division of Basic Pharmaceutical Sciences, College of Pharmacy, Xavier University of Louisiana, New Orleans, Louisiana, USA

[2]Department of Chemistry, RCMI Cancer Research Center, Xavier University of Louisiana, New Orleans, Louisiana, USA

Abstract

Human factor XIa (FXIa) is a serine protease in the intrinsic coagulation pathway. FXIa has been actively targeted to develop new anticoagulants that are associated with a reduced risk of bleeding. Thousands of FXIa inhibitors have been reported, yet none has reached the clinic thus far. We describe here a novel class of sulfonated molecules that allosterically inhibit FXIa with moderate potency. A library of 18 sulfonated molecules was evaluated for the inhibition of FXIa using a chromogenic substrate hydrolysis assay. Only six molecules inhibited FXIa with IC_{50} values of 4.6–29.5 μM. Michaelis–Menten kinetics indicated that sulfonated molecules are allosteric inhibitors of FXIa. Inhibition of FXIa by these molecules was reversed by protamine. The molecules also showed moderate anticoagulant effects in human plasma with preference to prolong activated partial thromboplastin time. Their binding to an allosteric site in the catalytic domain of FXIa was modeled to illustrate potential binding mode and potential important Arg/Lys residues. Particularly, inhibitor **16** (IC_{50} = 4.6 μM) demonstrated good selectivity over a panel of serine proteases including those in the coagulation process. Inhibitor **16** did not significantly compromise the viability of three cell lines. Overall, the reported sulfonated molecules serve as a new platform to design selective, potent, and allosteric inhibitors of FXIa for therapeutic applications.

Keywords

anticoagulants; factor XIa; heparin mimetics

Correspondence: Rami A. Al-Horani, College of Pharmacy, 1 Drexel Drive, New Orleans, LA 70125-1089, USA. ralhoran@xula.edu.

CONFLICT OF INTEREST

No conflict of interests is declared by the authors.

SUPPORTING INFORMATION

Additional supporting information may be found in the online version of the article at the publisher's website.

1 | INTRODUCTION

Anticoagulants are the keystone of the treatment and prevention of thromboembolic diseases, yet agents in clinics are linked to a significant risk of bleeding. This complicates their effective use in high-risk patients such as patients with atrial fibrillation or chronic kidney disease among others (Alamneh et al., 2016; Barra et al., 2016; Black-Maier & Piccini, 2017; Heine & Brandenburg, 2017; Hughes et al., 2014; Lutz et al., 2017). Heparin-based anticoagulants indirectly inhibit factor IIa (FIIa, also known thrombin) and/or factor Xa (FXa) via activating their endogenous serpin inhibitor, that is, antithrombin. Heparin-based anticoagulants have been used for decades; nevertheless, their multi-dimensional side effects including the risk of bleeding have always been a concern (Garcia et al., 2012). The indirect oral anticoagulant warfarin has also been used for years, yet it suffers from a narrow therapeutic window which demands permanent monitoring and frequent dose adjustment to lessen the risk of bleeding besides its other side effects (Jun et al., 2017; Kimachi et al., 2017; Larsen et al., 2016). Newer small molecule anticoagulants, including argatroban, dabigatran, rivaroxaban, apixaban, edoxaban, and betrixaban, directly inhibit thrombin or FXa (Ageno et al., 2012; Chan & Weitz, 2019; Garcia et al., 2012). They have been found to be effective with a relatively lesser bleeding risk than heparins and warfarin (Deitelzweig et al., 2018; Hellenbart et al., 2017; Jun et al., 2017). Nevertheless, additional decrease in the bleeding risk continues to be a necessity.

A promising drug target in the coagulation cascade to address the bleeding problem is factor XIa (FXIa). FXIa amplifies FIIa generation and contributes to the stabilization of fibrin by the progressive activation of factor IX and factor X (Al-Horani, 2020a, 2020b; Al-Horani & Afosah, 2018). Importantly, FXIa significantly contributes to the pathological clot formation, that is, thrombosis but plays only a minor role in the physiological blood clot formation, that is, hemostasis (Gailani et al., 2015; Mohammed et al., 2018). This suggested that inhibiting FXIa is likely to result in effective protection against thrombosis and is less likely to lead to bleeding complications. In fact, human epidemiological and animal data have supported such notion. Individuals with hemophilia C [congenital deficiency of factor XI (FXI)] appear to be less predisposed to venous thromboembolism and ischemic stroke and exhibit no elevated bleeding risk (Duga & Salomon, 2013; Salomon et al., 2008, 2011). Moreover, other studies have indicated that increased FXI activity correlates with a higher prevalence of venous thromboembolism and ischemic stroke (Gomez & Bolton-Maggs, 2008; Meijers et al., 2000; Suri et al., 2010; Undas et al., 2011, 2012).

In animal studies, reducing FXI level in knockout species, or by the use of antisense oligonucleotides that inhibit the hepatic biosynthesis of FXI or by the use of monoclonal antibodies that inhibit FXI(a) activity or activation has protected the animals against venous and arterial thrombosis without leading to an increased risk of bleeding (Al-Horani, 2020a, 2020b; Al-Horani & Afosah, 2018; Crosby et al., 2013; Ely et al., 2018; Wang et al., 2006). The antisense oligonucleotide IONIS FXI_{Rx} was the first FXI(a)-targeting agent to be studied for venous thromboembolism prevention in patients during total knee arthroplasty procedure (Büller et al., 2015). Reducing FXI level by IONIS FXI_{Rx} decreased the postoperative risk of venous thromboembolism compared with enoxaparin, a heparin -based anticoagulant, without substantially increasing bleeding risk (Büller et al., 2015).

Orthosteric small molecule inhibitors of FXIa have also been developed (Al-Horani, 2020a, 2020b; Al-Horani & Afosah, 2018; Beale et al., 2021; Dilger et al., 2022; Kubitza et al., 2022; Wong et al., 2022). In fact, the reporting of X-ray crystal structures of FXI(a) has contributed to structure- and ligand-based drug design (Fradera et al., 2012; Jin et al., 2005). FXI is a homodimer of two 80,000 Da subunits, each of which contains four apple (A) domains and a trypsin-like catalytic domain (Emsley et al., 2010; McMullen et al., 1991; Meijers et al., 1992). On the one hand, the four apple domains (A1–A4) contain binding sites for other proteins: thrombin in A1 domain, high-molecular-weight kininogen in A2 domain, the physiological substrate FIX, heparin, and glycoprotein Ib in A3 domain, and factor XIIa (FXIIa) in A4 domain. On the other hand, the active site of the catalytic domain contains the catalytic triad of H413, D462, and S557, as well as several substrate selectivity subsites. Furthermore, the catalytic domain contains an anion-binding site, via which glycosaminoglycans such as heparins can allosterically inhibit FXIa. FXIa is produced from its zymogen FXI by the action of thrombin and FXIIa (Al-Horani, 2020a, 2020b; Al-Horani & Afosah, 2018; Emsley et al., 2010; Gailani & Smith, 2009). While there is no currently approved FXIa inhibitor in clinical use, recent reports of milvexian (Figure 1a) appear to be very promising (Dilger et al., 2022; Goodwin, 2022; Perera et al., 2022; Weitz et al., 2021; Wong et al., 2022). Milvexian is a competitive inhibitor that compromises the catalytic activity of FXIa by targeting its active site.

Another approach that has been actively researched is to target FXIa's allosteric anion-binding site(s) on the catalytic domain and/or on the A3 domain. In this arena, sulfated pentagalloyl glucopyranoside (SPGG; Al-Horani et al., 2015), sulfated *chiro*-inositol (SCI; Al-Horani, Abdelfadiel, et al., 2019), lignosulfonic acid sodium (LSAS; Kar et al., 2021), and benzyl tetraphosphonate (BTP; Kar et al., 2020) (Figure 1b) were reported as allosteric inhibitors of FXIa, potentially by targeting the allosteric anion-binding site in the catalytic domain. In previous studies, it was shown that this site is recruited by SPGG, SCI, BTP, LSAS, and heparin, all are negatively charged molecules, to allosterically inhibit FXIa which resulted in a significant anticoagulant effect (Al-Horani, Abdelfadiel, et al., 2019; Al-Horani et al., 2015; Kar et al., 2020, 2021). Importantly, given that this site is not conserved among the different clotting serine proteases, that is, thrombin and FXa among others, targeting this site led to a significantly selective anticoagulant effect, and thus, better margin of safety as well as less likelihood of bleeding complications.

Accordingly, the aim of this study was to advance BTP by investigating the anticoagulant potential of its chemical space using sulfonated molecules. We have decided to replace the phosphonate group with sulfonate groups as the latter better resembles heparin, a sulfated glycosaminoglycan that was previously reported as an allosteric inhibitor of FXIa (Al-Horani, Abdelfadiel, et al., 2019; Al-Horani et al., 2015; Kar et al., 2020, 2021), yet with much greater chemical stability as the sulfate group is not susceptible to hydrolysis by heparanase or heparinase, sulfatase, or phosphatase. In the current study, we report the discovery of an allosteric sulfonated molecule (inhibitor **16**) that is more potent and effective than BTP. We strongly believe sulfonated molecules represented by inhibitor **16** serves as an interesting platform for developing anticoagulants that are less likely to cause bleeding complications than the current standard of care.

2 | MATERIALS AND METHODS

2.1 | Materials

Molecules **1**–**5** and **11** were obtained from Sigma-Aldrich and Fisher Scientific. Other molecules were obtained following modified reported synthetic protocols (Al-Horani et al., 2021; Kassack et al., 2004; McCain et al., 2004; Trapp et al., 2007). For instance, the pure sodium salts were produced by SP Sephadex-Na cation exchange chromatography and then by Sephadex G10 size exclusion chromatography. Final products were obtained following 24 h-drying process. The molecules were characterized by ^{1}H-NMR and ^{13}C-NMR, and the chemical shifts were similar to reported values (Kassack et al., 2004; McCain et al., 2004; Trapp et al., 2007). NMR was recorded in DMSO-d_6 on Bruker 600 MHz NMR spectrometer. The molecules' purity was more than 95%. See Supplementary Information for representative synthetic schemes and characterization data.

Enzymes for the kinetics studies were obtained from multiple companies. Their activities were verified as instructed by the supplying vendor. Human plasma proteins including FXIIIa, FXIa, FXa, FIXa, FIIa (thrombin), and plasmin were purchased from Haematologic Technologies. Bovine α-chymotrypsin and bovine trypsin were purchased from Sigma-Aldrich. Human neutrophil elastase (HNE) was purchased from Elastin Products Company. Proteinase 3 and cathepsin G were purchased from Fisher Scientific. The chromogenic substrates including Spectrozymes PL, FIXa, FXa, and TH were purchased from Biomedica Diagnostics. Trypsin chromogenic substrate (S-2222) and FXIa chromogenic substrate (S-2366) were purchased from Diapharma. Other chromogenic substrates: S-7388 for cathepsin G, S-1384 for HNE, M4765 for proteinase 3, and *N*-succinyl Ala-Ala-Pro-Phe-*p*-nitroanilide for chymotrypsin were from Sigma-Aldrich. Dimethylcasein, dithiothreitol, and dansyl-cadaverine were purchased from Sigma-Aldrich. Stock solutions of thrombin, FXIa, plasmin, proteinase 3, cathepsin G, chymotrypsin, and trypsin were all prepared in 50 mM Tris-HCl buffer, pH 7.4, containing 0.1% PEG8000, 150 mM sodium chloride, and 0.02% Tween80. Stock solution of FXa was prepared in 20 mM Tris-HCl buffer, pH 7.4, containing 100 mM sodium chloride, 2.5 mM $CaCl_2$, 0.1% PEG8000, and 0.02% Tween80. Stock solution of FIXa was prepared in 20 mM Tris-HCl buffer, pH 7.4, containing 100 mM NaCl, 2.5 mM $CaCl_2$, 0.1% PEG8000, 0.02% Tween80, and 33% v/v ethyleneglycol. Stock solution of HNE was prepared by reconstituting 1 mg with 100 μl of 1:1 glycerol:0.2 M sodium acetate buffer with pH 5, which was then diluted using HEPES buffer, pH 7.4, containing 125 mM HEPES, 100 mM sodium chloride, and 0.125% Triton-X 100. FXIIIa's stock solution was prepared in 50 mM Tris-HCl, 1 mM $CaCl_2$, 100 mM sodium chloride, 0.02% Tween80, 0.1% PEG8000, and 2 mg/ml dimethylcasein.

Human plasma for coagulation assays was obtained from George King Bio-Medica for the clotting assays. Thromboplastin–D (PT reagent), APTT reagent containing ellagic acid, and 0.025 M solution of $CaCl_2$ were obtained from Thermo Fisher Scientific. Results were reproduced at least two times.

2.2 | Inhibition of FXIa in chromogenic substrate hydrolysis assay by sulfonated molecules

Direct inhibition of human FXIa was measured by the corresponding chromogenic substrate hydrolysis assay, as reported previously (Al-Horani, Abdelfadiel, et al., 2019; Al-Horani, Clemons, et al., 2019; Al-Horani et al., 2015; Kar et al., 2020, 2021), at 37° and pH 7.4. Each well of the microplate had 85 μl of the buffer to which 5 μl of sulfonated molecules and 5 μl of FXIa (~0.8 nM) were successively added. Following incubation, 5 μl of FXIa substrate (~350 μM) was then added and the residual FXIa activity was measured from the initial rate of increase in absorbance at λ_{405} nm. Relative residual FXIa activity at each concentration of the sulfonated molecule was calculated from the ratio of FXIa activity in its absence and presence. Logistic Equation 1 was used to fit the concentration dependence of residual FXIa activity to calculate IC_{50} (*x*-axis, the potency) and ΔY% (*y*-axis, the efficacy) of inhibition.

$$Y = Y_0 + \frac{Y_M - Y_0}{1 + 10^{(\log[I]_0 - \log IC_{50})(HS)}} \quad (1)$$

In Equation 1, IC_{50} is the concentration of the molecule that inhibits 50% of the enzyme activity, Y is the ratio of residual FXIa activity in the presence of inhibitor to that in its absence, Y_0 and Y_M are the minimum and maximum possible values of the fractional residual FXIa activity, and HS is the Hill slope. Y_0, Y_M, IC_{50}, and HS are calculated by the non-linear curve fitting of the data.

2.3 | Michaelis–Menten kinetics for the FXIa-mediated hydrolysis of the chromogenic substrate S-2366 in the presence of inhibitor 14

The initial rate of S-2366 hydrolysis by pure human plasma FXIa was deduced from the linear increase in absorbance at λ_{405} nm corresponding to hydrolyzing less than 10% of S-2366, as indicated in earlier studies (Al-Horani, Abdelfadiel, et al., 2019; Al-Horani, Clemons, et al., 2019; Al-Horani et al., 2015; Kar et al., 2020, 2021). At 37°C, the initial rate was measured as a function of different concentrations of S-2366 (0–1500 μM) in the presence of a fixed concentration of inhibitor **14** in 20 mM Tris-HCl buffer of pH 7.4, containing 0.1% PEG8000, 0.15 M sodium chloride, and 0.02% Tween80. The study was performed in the presence of four concentrations of the inhibitor: 0, 4, 40, and 200 μM. The measurements were fitted using Michaelis–Menten Equation 2 to calculate K_M (*x*-axis, the affinity of the substrate to FXIa active site) and V_{MAX} (*y*-axis, the ceiling reaction velocity).

$$V = \frac{V_{MAX}[S]}{K_M + [S]} \quad (2)$$

2.4 | Selectivity studies against other serine proteases

The inhibition potential of several sulfonated molecules against thrombin, FXa, FIXa, plasmin, trypsin, chymotrypsin, cathepsin G, HNE, and proteinase 3 was also investigated using previously reported chromogenic substrate hydrolysis assays (Al-Horani, Abdelfadiel,

et al., 2019; Al-Horani, Clemons, et al., 2019; Al-Horani et al., 2015, 2021; Kar et al., 2020, 2021). For example, to each well of a 96-well microplate containing 85 μl or 185 μl of 20–50 mM Tris-HCl buffer, pH 7.4, containing 100–150 mM NaCl, 0.1% PEG8000, and 0.02% Tween80 at either 25°C or 37°C was added 5 μl of the inhibitor (or high pure water) and 5 μl of the enzyme. The final concentrations of the enzymes were 6 nM (thrombin), 89 nM (FIXa), and 1.09 nM (FXa). Following 10-min incubation, 5 μl of Spectrozyme TH (final conc. 0.050 mM), Spectrozyme FXa (0.125 mM), or Spectrozyme FIXa (0.85 mM) was rapidly added and the residual enzyme activity was measured from the initial rate of increase in absorbance at λ_{405} nm. Relative residual enzyme activity as a function of the concentration of the inhibitor was calculated. If 50% or more of the enzyme was inhibited, results were then plotted using Equation 1 to calculate the corresponding IC_{50} values.

2.5 | Selectivity study against FXIIIa

To measure the effect of sulfonated molecules on human FXIIIa, a previously reported fluorescence-based trans-glutamination assay was used (Al-Horani et al., 2016; Kar et al., 2020, 2021). In general, 1 μl of the inhibitor was added to 87 μl of 50 mM Tris-HCl buffer of pH 7.4, containing 100 mM sodium chloride, 1 mM $CaCl_2$, and 2 mg/ml dimethylcasein at 37°C. Afterward, 5 μl of dithiothreitol (0.02 M) and 2 μl of human FXIIIa (0.3 μM) were added, and the resulting mixture was incubated for 10 min. Following the addition of 5 μl of dansylcadaverine (2 mM), FXIIIa activity was obtained by measuring the initial rate of increase in fluorescence emission (excitation wavelength is 360 nm, and emission wavelength is 490 nm). The relative residual activity of FXIIIa was then calculated as a function of the inhibitor concentration. If 50% or more of the enzyme was inhibited, results were then plotted using Equation 1 to calculate the corresponding IC_{50} values.

2.6 | Reversibility studies

To evaluate the in vitro reversibility of inhibitory effects of this class of molecules, the profiles of restored FXIa activity were obtained using an increasing concentration of protamine in the presence of inhibitor **13** (80 μM) or inhibitor **14** (120 μM), as reported previously (Al-Horani et al., 2015). At pH 7.4 and 37°C, the measurement was performed by the S-2366 hydrolysis assay using the 96-well microplate reading platform. In general, each well of the microplate had 80 μl of 50 mM Tris-HCl buffer of pH 7.4 containing 0.1% PEG8000, 0.15 M sodium chloride, and 0.02% Tweeen80 to which 5 μl of the inhibitor (or vehicle), 5 μl of FXIa (~0.8 nM), and 5 μl of protamine were sequentially added. After incubation, 5 μl of S-2366 (~0.35 mM) was added and the restored activity of FXIa was obtained from the initial rate of increase in absorbance at λ_{405} nm. The relative restored activity of FXIa at each protamine concentration was calculated from the ratio of FXIa activity in the absence and presence of protamine. Logistic equation 3 was used to fit the data so as to obtain the effective concentration of protamine needed to restore 50% of the enzyme activity at certain inhibitor concentration (EC_{50}) and the efficacy (ΔY) of the activity restoration process.

$$Y = Y_0 + \frac{Y_M - Y_0}{1 + 10^{(\log[R]_0 - \log EC_{50})(HS)}} \quad (3)$$

2.7 | Effect of sulfonated molecules on the clotting of normal human plasma

Clotting times (APTT and PT) in normal human plasma were measured using the BBL Fibrosystem fibrometer (Becton–Dickinson), as previously reported (Al-Horani, Abdelfadiel, et al., 2019; Al-Horani, Clemons, et al., 2019; Al-Horani et al., 2015, 2021; Kar et al., 2020, 2021). For the APTT assay, 10 μl of the inhibitor was mixed with 90 μl of citrated human plasma and 100 μl of prewarmed APTT reagent (0.2% ellagic acid). After incubation for 240 s at 37°C, clotting was initiated by adding 100 μl of prewarmed 0.025 M $CaCl_2$, and the time to clotting was recorded. For the PT assay, thromboplastin-D was dissolved in 4 ml of highly purified water, and the resulting mixture was then warmed to 37°C. A 10 μl of the inhibitor was then added to 90 μl of normal human plasma and was next incubated for 30 s. After the addition of 200 μl of prewarmed PT reagent, the time to clotting was noted. Several concentrations of the inhibitor were used in the two assays to construct a concentration vs effect curve. The data were fitted to a quadratic trend line, which was ultimately used to calculate the concentration of the inhibitor needed to prolong the plasma clotting time by 1.5-fold. Using 10 μl of deionized water, clotting times of normal human plasma in the absence of an anticoagulant were determined to be 32.4 ± 0.2 s for APTT and 12.4 ± 1.0 s for PT.

2.8 | The cellular toxicity of inhibitor 16 (effect on cell viability)

CaCo-2 heterogeneous human epithelial colorectal adenocarcinoma cells (Lea, 2015), HEK-293 human embryonic kidney cells (Lin et al., 2014), and MCF-7 human breast carcinoma cells (Comşa et al., 2015) were treated as described previously (Burow et al., 2001; Liu et al., 2015). The test was performed by the CMB core of the XULA's RCMI Program via a modified procedure using Alamar Blue (resazurin) fluorescent dye (Burow et al., 2001; Liu et al., 2015). Briefly, CaCo-2, HEK-293, and MCF-7 cells were seeded in a 96-well plate at an optimized conditions to achieve the log growth phase. The plates were kept covered during the experiment to guarantee their sterility. Alamar Blue dye was added to each well, and then, the plates were incubated for 2 h at 37°C. Th plates were read in a fluorescence mode (excitation wavelength 560 nm and emission wavelength 590 nm) on the Synergy H1 multiplate reader (BioTek) to determine the number of cells in the absence (distilled water was used as control) or the presence of inhibitor **16** (90 μM; 3 days incubation). Distilled water control was used to ensure that the observed effect was because of the inhibitors. The measurements were repeated four times to obtain the standard deviations.

2.9 | Molecular modeling studies of inhibitors 13, 15, and 16 and human FXIa

The studies were performed using Glide of Schrodinger Suite 2017–1 (Schrödinger, 2017). FXIa coordinates were obtained from the crystal structure of α-ketothiazole arginine-based ligand—FXIa complex (PDB: 2FDA; Deng et al., 2006). The protein was prepared by eliminating the crystal ligand and the crystallographic water molecules, and by introducing H atoms in harmony with pH 7.0 using Schrodinger Suite Maestro 11.1. The protein structure was energetically minimized with 0.3 Å as the cutoff value of RMSD for all heavy atoms. Likewise, the coordinates of the inhibitors were built and energetically minimized. The ligand-binding site was defined to include the basic residues K179, K175, R173, R171,

K170, N165, and T164 (chymotrypsin numbering) in the catalytic domain and their vicinity. The protein grids were produced by the OPLS3 forcefield (Harder et al., 2016). The center of the grid was determined to be the centroid of the above residues, with a grid box of 10 Å on each side. No constraints were used in the grid generations. The calculations were performed using the default values in the standard precision mode. The resulting poses were also minimized. The best-docked structure, that is, best score was chosen for further analysis.

3 | RESULTS AND DISCUSSION

3.1 | Direct inhibition of human FXIa by sulfonated molecules (1–18)

A library of 18 sulfonated molecules (Figure 2) was evaluated for FXIa inhibition using the corresponding tripeptide chromogenic substrate (S-2366) hydrolysis assay in pH 7.4 Tris-HCl buffer at 37°C, as reported previously (Al-Horani, Abdelfadiel, et al., 2019; Al-Horani, Clemons, et al., 2019; Al-Horani et al., 2015; Kar et al., 2020, 2021). The structures of molecules are diverse considering the size, shape, and number of sulfonate groups. They include aminobenzene sulfonic acid (**1**) and its *N*-benzoyl derivatives (**6** and **7**), amino-naphthalene sulfonic acid derivatives (**2**–**5**) and their *N*-benzoyl derivatives (**8**–**10**), di-sulfonated dinaphthyl urea derivative (**11**), and variably sulfonated diphenyl urea derivatives (**12**–**18**). The molecules have different number of sulfonate groups: one group (**1**, **2**, **6**, and **7**), two (**3**, **4**, and **11**), three (**5** and **8**–**10**), four (**12** and **17**), six (**13**–**16**), and eight (**18**). The dinaphthyl urea derivative (**11**) and all diphenyl urea derivatives (**12**–1**8**) are symmetrical with either a linear shape (**11**–**16**) or a globular shape (**17** and **18**). The extended diphenyl-urea derivatives have either short linker (**12** and **13**) or longer linker (**14**–**16**). Such diversity is important in exploring the chemical space surrounding the previously published inhibitor BTP.

In the used assay, the catalytic activity of FXIa is determined by measuring the initial hydrolysis rate of S-2366 as provided by the absorbance at λ_{405} nm. The fractional decrease in the initial hydrolysis rate of the chromogenic substrate S-2366 in the presence of an inhibitor is examined using the logistic Equation 1 to determine its potency (x-axis, IC_{50}) and efficacy (y-axis, ΔY%) (see Section 2). Figure 3 shows representative semilog inhibition curves observed for inhibitors **14**–**17**. Only six molecules concentration-dependently inhibited FXIa. Other molecules did not inhibit FXIa at the highest concentrations studied. The range of inhibitory potency was found to be relatively mediocre (4.6–29.5 μM), whereas the efficacy for all inhibitors was superior (>87%; Table 1).

Critical structure–activity relationship points can be obtained from this exercise. First, the number of sulfonates appears to be marginally important although the sulfonate group itself appears to be inherently essential for FXIa inhibition. Even though the most potent inhibitor is the hexa-sulfonated derivative **16** (IC_{50} = 4.6 μM), substantial inhibition is also obtained by di -and tetra -sulfonated derivatives **11** and **17** (IC_{50} values are 24.5 and 29.5 μM, respectively). Second, sulfonated diphenyl-urea derivatives with shorter linkers are less potent than related molecules with extended linkers (inhibitors **13** is ~twofold less potent than inhibitors **14** and **15**). Third, globular molecules appear to have better

inhibition potency than linear molecules with the same number of sulfonate groups. For example, the globular tetra-sulfonated inhibitor **17** is >17-fold more potent than the linear tetra-sulfonated molecule **12**. Interestingly, there appear to be a maximally favorable number of sulfonate groups on a globular molecule to bring about a meaningful inhibition of FXIa as evidently demonstrated by molecules **17** (tetra-sulfonated; IC_{50} = 29.5 μM) and **18** (octa-sulfonated; IC_{50} > 500 μM). Furthermore, replacement of methyl substituents with fluorine substituents increases the potency by ~twofold, as exhibited by inhibitors **14** and **15**. This is likely because the fluorine substituents de-solvate the sulfonate groups on the same molecules, and thus, make them available to bind to the corresponding amino acid on FXIa. Lastly, by comparing the potency of inhibitors **14** and **15** with that of inhibitor **16**, it becomes obvious that the optimal position for the tri-sulfonated naphthalene-4-formamido(benzamido) moiety, with respect to the urea group, is the *para*-position. Indeed, inhibitor **16** is ~twofold and ~fourfold more potent than inhibitors **14** and **15**, respectively, although all three inhibitors are hexa-sulfonated derivatives. Together, the most potent inhibitor discovered in this study is the hexa-sulfonated molecule **16** which 100% inhibited FXIa with potency of 4.6 μM. These numbers are much better than those of BTP which only 68% inhibited FXIa with potency of 7.4 μM (Kar et al., 2020).

3.2 | Michaelis–Menten kinetics of the hydrolysis of the chromogenic substrate S-2366 by FXIa in the presence of inhibitor 14

To shed light on the mechanistic aspects of FXIa inhibition by sulfonated molecules, Michaelis–Menten kinetics of S-2366 hydrolysis by FXIa was done in the presence of inhibitor **14** under physiological conditions. Figure 4 exhibits the initial rate profiles in the presence of inhibitor **14** (0–200 μM). The profiles show characteristic rectangular hyperbolic trends, which could be fitted using Equation 2 to obtain the apparent K_M (substrate apparent affinity) and V_{MAX} (maximum velocity) (Table 2). The K_M value for S-2366 did not significantly change (0.31 ± 0.03 mM–0.32 ± 0.11 mM) in the absence or presence of inhibitor **14**. However, the V_{MAX} decreased from 40.0 ± 1.3 mAU/min in the absence of inhibitor **14** to 12.9 ± 1.6 mAU/min at 200 μM of inhibitor **14**. Thus, the inhibitor appears not to affect the formation of Michaelis complex; however, it may cause conformational changes in the active site of FXIa that disrupts its catalytic activity. This indicates that molecule **14** inhibits FXIa in allosteric fashion.

3.3 | Selectivity studies: inhibition of coagulation, inflammation, fibrinolysis and digestive proteins by sulfonated molecules

To study the selectivity of the sulfonated inhibitors of FXIa, we first tested all active ones against thrombin and FXa, the two serine proteases that are being targeted by the current anticoagulants. The activity of sulfonated molecules toward thrombin and FXa was studied using appropriate chromogenic substrate hydrolysis assays, as reported previously (Al-Horani, Abdelfadiel, et al., 2019; Al-Horani, Clemons, et al., 2019; Al-Horani et al., 2015, 2021; Kar et al., 2020, 2021). In these assays, the inhibition potential was determined by spectrophotometric measurement of the residual protease activity in the presence of varying concentrations of sulfonated molecules (Table 3). In this arena, inhibitor **11** was found not to inhibit thrombin or FXa at the highest concentration tested of 100 μM,

demonstrating at least fourfold of selectivity. Inhibitor **13** demonstrated a selectivity index of at least 20-fold over thrombin and ~3.5-fold over FXa, although it only inhibited the latter by ~52% at the highest concentration tested of 500 μM. Although molecule **14** inhibited thrombin and FXa, but its efficacy was only ~53% against thrombin and ~77% against FXa, where it was more effective inhibitor against FXIa with efficacy of ~90%. Molecule **15** inhibited FXIa with twofold (albeit with low efficacy of ~40%) and 20-fold selectivity over thrombin and FXa, respectively. The most promising case was demonstrated by inhibitor **16** which exhibited >22-fold selectivity toward FXIa over thrombin and ~11-fold selectivity toward FXIa over FXa (Figure 5). Inhibitor **17** demonstrated a selectivity index of at least threefold over the two proteins.

Furthermore, inhibitors **13**, **14**, and **16** were also evaluated against one or more of the following enzymes: Factor IXa (FIXa), factor XIIIa (FXIIIa), HNE, proteinase 3, cathepsin G, plasmin, chymotrypsin, and trypsin. Except for FXIIIa, all other enzymes are serine proteases, and thus, the activity of sulfonated molecules toward any one of them was performed using previously reported chromogenic substrate hydrolysis assays (Al-Horani et al., 2015, 2021; Al-Horani, Abdelfadiel, et al., 2019; Al-Horani, Clemons, et al., 2019; Kar et al., 2020, 2021). In the above assays, the inhibition potential was investigated by spectrophotometrically measuring the residual activity of the protease in the presence of different concentrations of inhibitors **13**, **14**, or **16** (Tables 4 and 5). For FXIIIa, the molecules' activity was investigated using a previously reported fluorescence-based trans-glutamination test (Al-Horani et al., 2016; Kar et al., 2020, 2021). The above assays with the other enzymes indicated that the three molecules demonstrated selectivity indices of 6.5-fold, 4.5-fold, and 18-fold, respectively, toward FXIa over FXIIIa. Inhibitor **16** also exhibited a selectivity index of 76-fold toward FXIa over FIXa (Figure 5). The three molecules also demonstrated substantial selectivity over plasmin, trypsin, and chymotrypsin (Table 5). Interestingly, all three molecules inhibited HNE, although with variable potency. In fact, molecule **16** potently inhibited the inflammatory enzyme HNE with a potency of 0.22 μM. Not only that, but it also inhibited two other inflammatory enzymes cathepsin G and proteinase 3 with IC_{50} values of 0.57 and 34.2 μM, respectively (Table 5).

Overall, it appears that the most potent and selective molecule in the library is inhibitor **16**. Using the highest concentration tested of inhibitor **16** against the above enzymes, the calculated IC_{50} values were determined to be >350 μM for FIXa, ~49 μM for FXa, >100 μM for FIIa, and ~84 μM for FXIIIa (Table 4), and by considering the FXIa IC_{50} of 4.6 μM, inhibitor **16** is associated with selectivity indices of >22-fold, ~11-fold, >76-fold, and ~18-fold, respectively, over coagulation proteins. Also, it did exhibit selectivity indices of >39-fold over the fibrinolysis enzyme plasmin as well as the digestive enzymes trypsin and chymotrypsin. Interestingly, however, molecule **16** potently inhibited the inflammatory proteins alluding to the potential of developing a dual-acting molecule possessing anticoagulant and anti-inflammatory properties.

3.4 | Reversibility by cationic polymer, protamine

An important consideration while developing new anticoagulants is reversibility. To determine whether FXIa inhibition by sulfonated molecules can be reversed, we considered

protamine which is a clinically used arginine-rich polypeptide that reverses the anticoagulant activity of unfractionated heparin and low molecular weight heparins (Al-Horani et al., 2015). FXIa was first treated with inhibitor **13** (80 μM) or inhibitor **14** (120 μM), and the restoration of FXIa activity by protamine studied spectrophotometrically through the hydrolysis of S-2366 (Figure 6). The efficacy and the effective concentration of protamine to restore 50% of enzyme activity (EC_{50}) were found to be ~72% and 289.3 μg/ml, respectively, for inhibitor **13** and ~74% and 599 μg/ml, respectively, for inhibitor **14**. An important aspect that can be inferred from this exercise is that the interactions between these inhibitors and FXIa are ionic or polar (H-bond) in nature and stem from the interactions between the negative charged groups on the molecules, that is, sulfonate groups and the positively charged amino acids of the binding site on FXIa, potentially Lys and Arg residues in the anion-binding site of the catalytic domain as reported for other allosteric inhibitors (Al-Horani, Abdelfadiel, et al., 2019; Al-Horani, Clemons, et al., 2019; Al-Horani et al., 2015; Kar et al., 2021).

3.5 | Effects on activated partial thromboplastin time (APTT) and prothrombin time (PT) in normal human plasma

Plasma clotting assays are commonly used to study the antithrombotic potential of new clotting enzyme inhibitors. The APTT evaluates the effect of potential anticoagulants on the contact/intrinsic pathway-mediated clotting which involves factors XIIa, XIa, and IXa. The PT evaluates the effect of potential anticoagulant on the extrinsic pathway of coagulation which mainly involves FVIIa. Thus, we evaluated the effect of the sulfonated molecules on APTT and PT of human plasma, as reported previously (Al-Horani et al., 2015, 2021; Al-Horani, Abdelfadiel, et al., 2019; Al-Horani, Clemons, et al., 2019; Kar et al., 2020, 2021). Reported in Table 6 are the concentrations of inhibitors **13**–**17** that are required to increase each time by 1.5-fold. Although the activity of molecules appears to be mediocre of micro-molar concentration range, results suggest a preferential effect on APTT which entails FXIa.

3.6 | The cellular toxicity of inhibitor 16

To evaluate the cellular toxicity of inhibitor **16**, its anti-proliferative properties were studied in three cell lines of intestine (CaCo-2), breast (MCF-7), and kidney (HEK-293), as described earlier (Burow et al., 2001; Liu et al., 2015). Results suggested that 90 μM of the inhibitor (~20-fold of the IC_{50}) does not substantially affect the proliferation of the above cell lines. Overall, inhibitor **16** is a promising lead for further development as a selective, allosteric, and nontoxic inhibitor of FXIa. As a proof-of-concept, 300 μM of inhibitor **17** does not affect the proliferation of any of the three cell lines.

3.7 | Molecular modeling studies

To devise plausible binding mode(s) for sulfonated molecules, we conducted molecular docking studies considering the anion-binding site on the catalytic domain of FXIa. The justification for targeting this site is that its Arg and Lys residues are involved in FXI(a) interactions with the negatively charged functional groups of several macromolecules including the phosphates of inorganic polyphosphates (Yang et al., 2009) and the sulfates of

heparins (Geng et al., 2013). The same site is also involved in the action of SCI and that of SPGG, two glycosaminoglycan mimetics that were reported as allosteric FXIa inhibitors (Al-Horani, Abdelfadiel, et al., 2019; Al-Horani et al., 2015). The docking studies of three sulfonated molecules, namely **13**, **15**, and **16**, onto the anion-binding site were performed using Glide (Schrödinger, 2017). Coordinates for FXIa's catalytic domain were obtained from the protein databank (PDB ID: 2FDA; Deng et al., 2006). The docking exercises indicated that the three molecules adopted different binding modes, with similar interactions on one naphthalene end of the symmetrical structures, and distinct ones for the linkers and the other naphthalene ends of the molecules. In particular, the studies revealed that two sulfonate groups on one naphthalene end of all three inhibitor structures interact via electrostatic/H-bond with K170 and R185 (Figure 7a–c). Nevertheless, one of the amide linkers of inhibitor **13** H-bonds with T164 while the carbonyl oxygen of its urea central domain H-bonds with the backbone amine of E166 (Figure 7a). For inhibitor **15**, one of the amide linkers H-bonds with the backbone amine of L162 (Figure 7b). In inhibitor **16**, one of the amide linkers H-bonds with the guanidine group of R173 (Figure 7c), which is very substantial. Subtle differences are exhibited by interactions of the other naphthalene end of the symmetrical molecules **13**, **15**, and **16**. Inhibitor **13** is shorter molecule, and thus, one sulfonate interacts with K175 via electrostatic/H-bond. Inhibitor **15**, however, reaches further and one of its sulfonate groups interacts with H178 and K179 while another sulfonate H-bonds with Y101. More importantly, the most potent inhibitor, which is molecule **16**, showed more interactions. One of its sulfonate groups interacts with H178 and K179 while another sulfonate H-bonds with Q93 and Y101.

Together, inhibitor **13** interacts with T164, E166, K170, K175, and R185; inhibitor **15** interacts with Y101, L162, K175, H178, K179, and R185; and lastly, inhibitor **16** interacts with Q93, Y101, R173, K175, H178, K179, and R185. This pattern of interactions is in line with the measured potency of the three molecules; inhibitor **16** is more potent than inhibitor **15**, which is in turn more potent than inhibitor **13**. It is worth to mention here that several of the above residues are involved in heparin-facilitated inhibition of FXIa by antithrombin (Geng et al., 2013) and in polyphosphate-facilitated activation of FXI by thrombin and FXIIa (Yang et al., 2009) which explains the potency of the above inhibitors, particularly inhibitor **16**. Furthermore, several of those residues are involved in FXIa inhibition by BTP (Kar et al., 2020). Importantly, these results highlight that at least four sulfonate groups are needed to substantially inhibit FXIa. Although the above results are to be confirmed by mutagenesis studies and/or crystallography experiments, they are important as the identified binding modes can be exploited to direct future efforts to optimize the selectivity and the potency of inhibitor **16**.

4 | CONCLUSION AND FUTURE DIRECTIONS

We identified a new class of allosteric and sulfonated inhibitors of human FXIa. We previously identified BTP as a tetraphosphonated allosteric inhibitor of FXIa with potency of ~7.4 μM and an efficacy of ~68% (Kar et al., 2020). In this study, we identified sulfonated inhibitor **16** as selective, allosteric, and sulfonated inhibitor of FXIa with potency of ~4.6 μM and near complete efficacy (Table 1; Figure 3). The molecule exhibited

significant selectivity over other coagulation, fibrinolysis, and digestive enzymes. We expect that this inhibitor will serve as an excellent lead to guide future development of sulfonated allosteric inhibitors of FXIa as a new generation of anticoagulants that are not associated with hemorrhage risk. Such chemotype of inhibitors is expected to offer the following advantages: (1) they are homogeneous molecules that are potentially less susceptible to hydrolytic enzymes that target similar allosteric inhibitors, including sulfatase and heparanase; (2) they are unlikely to pass through the placenta or blood–brain barrier given their anionic nature, and this further demonstrates their safety; (3) they do not impact the proliferation of various cell lines suggesting a higher index of safety; and (4) they can be developed as prodrugs to increase their oral bioavailability (Yan & Müller, 2004). Furthermore, these inhibitors will be very suitable for in-hospital use as well as emergency use given their amenability to parenteral administration owing to their high solubility in water.

Given the low risk of bleeding, FXIa inhibitors are set to serve a wider range of thrombotic patients, especially patients at a higher risk of both thrombosis and bleeding such as patients with atrial fibrillation and those with chronic kidney diseases (Alamneh et al., 2016; Barra et al., 2016; Black-Maier & Piccini, 2017; Heine & Brandenburg, 2017; Hughes et al., 2014; Lutz et al., 2017). Interestingly, inhibitor **16** was also found to potently inhibit cathepsin G and HNE, and to moderately inhibit proteinase 3 (Table 5). Therefore, inhibitor **16** can serve as a novel platform to develop dual-acting agents with anticoagulant and anti-inflammatory properties, without disrupting normal hemostasis. These agents may be proved beneficial in treating complex pathologies, in which coagulation and inflammation play major roles such as sepsis, disseminated intravascular coagulation, colitis, pneumonitis, arthritis, ischemic stroke, and diabetic nephropathy (Foley & Conway, 2016). Lastly, inflammation and coagulation are important driving forces in exacerbating infectious diseases as demonstrated by the ongoing pandemic of COVID-19 (Al-Horani, 2020a, 2020b; Aliter & Al-Horani, 2021a, 2021b). Thus, inhibitor **16** and similar molecules may hold a potential in treating the severe cases of COVID-19 infection. This remains to be tested.

Supplementary Material

Refer to Web version on PubMed Central for supplementary material.

ACKNOWLEDGEMENTS

The study reported was supported by a grant from the US National Institute of General Medical Sciences (NIGMS) to RAAH under award number SC3GM131986 and by a grant from the US National Institute on Minority Health and Health Disparities (NIMHD) to MM under award number U54MD007595. The content is solely the responsibility of the authors and does not necessarily represent the official views of the funding institutions. We would like to thank Dr. Edward Ofori of Chicago State University and Dr. Thomas Wiese of Xavier University of Louisina for their technical support.

Funding information

National Institute on Minority Health and Health Disparities; National Institute of General Medical Sciences

REFERENCES

Ageno W, Gallus AS, Wittkowsky A, Crowther M, Hylek EM, & Palareti G (2012). Oral anticoagulant therapy: Antithrombotic therapy and prevention of thrombosis, 9th ed: American College of Chest Physicians Evidence-Based Clinical Practice Guidelines. Chest, 141(2 Suppl), e44S–e88S. 10.1378/chest.11-2292 [PubMed: 22315269]

Alamneh EA, Chalmers L, & Bereznicki LR (2016). Suboptimal use of oral anticoagulants in atrial fibrillation: Has the introduction of direct oral anticoagulants improved prescribing practices? American Journal of Cardiovascular Drugs: Drugs, Devices, and Other Interventions, 16(3), 183–200. 10.1007/s40256-016-0161-8 [PubMed: 26862063]

Al-Horani RA (2020a). Factor XI(a) inhibitors for thrombosis: An updated patent review (2016-present). Expert Opinion on Therapeutic Patents, 30(1), 39–55. 10.1080/13543776.2020.1705783 [PubMed: 31847619]

Al-Horani RA (2020b). Potential therapeutic roles for direct factor Xa inhibitors in coronavirus infections. American Journal of Cardiovascular Drugs, 20(6), 525–533. 10.1007/s40256-020-00438-6 [PubMed: 32918208]

Al-Horani RA, Abdelfadiel EI, Afosah DK, Morla S, Sistla JC, Mohammed B, Martin EJ, Sakagami M, Brophy DF, & Desai UR (2019). A synthetic heparin mimetic that allosterically inhibits factor XIa and reduces thrombosis in vivo without enhanced risk of bleeding. Journal of Thrombosis and Haemostasis, 17(12), 2110–2122. 10.1111/jth.14606 [PubMed: 31397071]

Al-Horani RA, & Afosah DK (2018). Recent advances in the discovery and development of factor XI/XIa inhibitors. Medicinal Research Reviews, 38(6), 1974–2023. 10.1002/med.21503 [PubMed: 29727017]

Al-Horani RA, Aliter KF, Kar S, & Mottamal M (2021). Sulfonated nonsaccharide heparin mimetics are potent and noncompetitive inhibitors of human neutrophil elastase. ACS Omega, 6(19), 12699–12710. 10.1021/acsomega.1c00935 [PubMed: 34056422]

Al-Horani RA, Clemons D, & Mottamal M (2019). The in vitro effects of pentamidine isethionate on coagulation and fibrinolysis. Molecules, 24(11), 2146. 10.3390/molecules2112146

Al-Horani RA, Gailani D, & Desai UR (2015). Allosteric inhibition of factor XIa. Sulfated non-saccharide glycosaminoglycan mimetics as promising anticoagulants. Thrombosis Research, 136(2), 379–387. 10.1016/j.thromres.2015.04.017 [PubMed: 25935648]

Al-Horani RA, Karuturi R, Lee M, Afosah DK, & Desai UR (2016). Allosteric inhibition of factor XIIIa. Non-saccharide glycosaminoglycan mimetics, but not glycosaminoglycans, exhibit promising inhibition profile. PLoS One, 11(7), e0160189. 10.1371/journal.pone.0160189 [PubMed: 27467511]

Aliter KF, & Al-Horani RA (2021b). Potential therapeutic benefits of dipyridamole in COVID-19 patients. Current Pharmaceutical Design, 27(6), 866–875. 10.2174/1381612826666201001125604 [PubMed: 33001004]

Aliter KF, & Al-Horani RA (2021b). Thrombin inhibition by argatroban: Potential therapeutic benefits in COVID-19. Cardiovascular Drugs and Therapy, 35(2), 195–203. 10.1007/s10557-020-07066-x [PubMed: 32870433]

Barra ME, Fanikos J, Connors JM, Sylvester KW, Piazza G, & Goldhaber SZ (2016). Evaluation of dose-reduced direct oral anticoagulant therapy. The American Journal of Medicine, 129(11), 1198–1204. 10.1016/j.amjmed.2016.05.041 [PubMed: 27341955]

Beale D, Dennison J, Boyce M, Mazzo F, Honda N, Smith P, & Bruce M (2021). ONO-7684 a novel oral FXIa inhibitor: Safety, tolerability, pharmacokinetics and pharmacodynamics in a first-in-human study. British Journal of Clinical Pharmacology, 87(8), 3177–3189. 10.1111/bcp.14732 [PubMed: 33450079]

Black-Maier E, & Piccini JP (2017). Oral anticoagulation in end -stage renal disease and atrial fibrillation: Is it time to just say no to drugs? Heart, 103(11), 807–808. 10.1136/heartjnl-2016-310540 [PubMed: 28069637]

Büller HR, Bethune C, Bhanot S, Gailani D, Monia BP, Raskob GE, Segers A, Verhamme P, Weitz JI, & FXI-ASO TKA Investigators. (2015). Factor XI antisense oligonucleotide for

prevention of venous thrombosis. The New England Journal of Medicine, 372(3), 232–240. 10.1056/NEJMoa1405760 [PubMed: 25482425]

Burow ME, Boue SM, Collins-Burow BM, Melnik LI, Duong BN, Carter-Wientjes CH, Li S, Wiese TE, Cleveland TE, & McLachlan JA (2001). Phytochemical glyceollins, isolated from soy, mediate antihormonal effects through estrogen receptor alpha and beta. The Journal of Clinical Endocrinology and Metabolism, 86(4), 1750–1758. 10.1210/jcem.86.4.7430 [PubMed: 11297613]

Chan NC, & Weitz JI (2019). Antithrombotic Agents. Circulation Research, 124(3), 426–436. 10.1161/CIRCRESAHA.118.313155 [PubMed: 30702990]

Comşa Ş, Cîmpean AM, & Raica M (2015). The story of MCF-7 breast cancer cell line: 40 years of experience in research. Anticancer Research, 35(6), 3147–3154. [PubMed: 26026074]

Crosby JR, Marzec U, Revenko AS, Zhao C, Gao D, Matafonov A, Gailani D, MacLeod AR, Tucker EI, Gruber A, Hanson SR, & Monia BP (2013). Antithrombotic effect of antisense factor XI oligonucleotide treatment in primates. Arteriosclerosis, Thrombosis, and Vascular Biology, 33(7), 1670–1678. 10.1161/ATVBAHA.113.301282 [PubMed: 23559626]

Deitelzweig S, Farmer C, Luo X, Li X, Vo L, Mardekian J, Fahrbach K, & Ashaye A (2018). Comparison of major bleeding risk in patients with non-valvular atrial fibrillation receiving direct oral anticoagulants in the real-world setting: A network meta-analysis. Current Medical Research and Opinion, 34(3), 487–498. 10.1080/03007995.2017.1411793 [PubMed: 29188721]

Deng H, Bannister TD, Jin L, Babine RE, Quinn J, Nagafuji P, Celatka CA, Lin J, Lazarova TI, Rynkiewicz MJ, Bibbins F, Pandey P, Gorga J, Meyers HV, Abdel-Meguid SS, & Strickler JE (2006). Synthesis, SAR exploration, and X-ray crystal structures of factor XIa inhibitors containing an alpha-ketothiazole arginine. Bioorganic & Medicinal Chemistry Letters, 16(11), 3049–3054. 10.1016/j.bmcl.2006.02.052 [PubMed: 16524727]

Dilger AK, Pabbisetty KB, Corte JR, De Lucca I, Fang T, Yang WU, Pinto DJP, Wang Y, Zhu Y, Mathur A, Li J, Hou X, Smith D, Sun D, Zhang H, Krishnananthan S, Wu D-R, Myers JE, Sheriff S, … Ewing WR (2022). Discovery of milvexian, a high-affinity, orally bioavailable inhibitor of factor XIa in clinical studies for antithrombotic therapy. Journal of Medicinal Chemistry, 65(3), 1770–1785. 10.1021/acs.jmedchem.1c00613 [PubMed: 34494428]

Duga S, & Salomon O (2013). Congenital factor XI deficiency: An update. Seminars in Thrombosis and Hemostasis, 39(6), 621–631. 10.1055/s-0033-1353420 [PubMed: 23929304]

Ely LK, Lolicato M, David T, Lowe K, Kim YC, Samuel D, Bessette P, Garcia JL, Mikita T, Minor DL Jr., & Coughlin SR (2018). Structural basis for activity and specificity of an anticoagulant anti-FXIa monoclonal antibody and a reversal agent. Structure, 26(2), 187–198.e4. 10.1016/j.str.2017.12.010 [PubMed: 29336885]

Emsley J, McEwan PA, & Gailani D (2010). Structure and function of factor XI. Blood, 115(13), 2569–2577. 10.1182/blood-2009-09-199182 [PubMed: 20110423]

Foley JH, & Conway EM (2016). Cross talk pathways between coagulation and inflammation. Circulation Research, 118(9), 1392–1408. 10.1161/CIRCRESAHA.116.306853 [PubMed: 27126649]

Fradera X, Kazemier B, Carswell E, Cooke A, Oubrie A, Hamilton W, Dempster M, Krapp S, Nagel S, & Jestel A (2012). High-resolution crystal structures of factor XIa coagulation factor in complex with nonbasic high-affinity synthetic inhibitors. Acta Crystallographica. Section F, Structural Biology and Crystallization Communications, 68(Pt 4), 404–408. 10.1107/S1744309112009037 [PubMed: 22505407]

Gailani D, Bane CE, & Gruber A (2015). Factor XI and contact activation as targets for antithrombotic therapy. Journal of Thrombosis and Haemostasis, 13(8), 1383–1395. 10.1111/jth.13005 [PubMed: 25976012]

Gailani D, & Smith SB (2009). Structural and functional features of factor XI. Journal of Thrombosis and Haemostasis, 7 (Suppl. 1), 75–78. 10.1111/j.1538-7836.2009.03414.x [PubMed: 19630773]

Garcia DA, Baglin TP, Weitz JI, & Samama MM (2012). Parenteral anticoagulants: Antithrombotic therapy and prevention of thrombosis, 9th ed: American College of Chest Physicians Evidence-Based Clinical Practice Guidelines. Chest, 141(2 Suppl.), e24S–e43S. 10.1378/chest.11-2291 [PubMed: 22315264]

Geng Y, Verhamme IM, Smith SA, Cheng Q, Sun M, Sheehan JP, Morrissey JH, & Gailani D (2013). Factor XI anion-binding sites are required for productive interactions with polyphosphate. Journal of Thrombosis and Haemostasis, 11(11), 2020–2028. 10.1111/jth.12414 [PubMed: 24118982]

Gomez K, & Bolton-Maggs P (2008). Factor XI deficiency. Haemophilia, 14(6), 1183–1189. 10.1111/j.1365-2516.2008.01667.x [PubMed: 18312365]

Goodwin NC (2022). Persistence pays off: Milvexian emerges from the industry's longstanding search for orally bioavailable factor XIa inhibitors. Journal of Medicinal Chemistry, 65(3), 1767–1769. 10.1021/acs.jmedchem.1c02108 [PubMed: 34962399]

Harder E, Damm W, Maple J, Wu C, Reboul M, Xiang JY, Wang L, Lupyan D, Dahlgren MK, Knight JL, Kaus JW, Cerutti DS, Krilov G, Jorgensen WL, Abel R, & Friesner RA (2016). OPLS3: A force field providing broad coverage of drug-like small molecules and proteins. Journal of Chemical Theory and Computation, 12(1), 281–296. 10.1021/acs.jctc.5b00864 [PubMed: 26584231]

Heine GH, & Brandenburg V (2017). Anticoagulation, atrial fibrillation, and chronic kidney disease-whose side are you on? Kidney International, 91(4), 778–780. 10.1016/j.kint.2016.11.028 [PubMed: 28314578]

Hellenbart EL, Faulkenberg KD, & Finks SW (2017). Evaluation of bleeding in patients receiving direct oral anticoagulants. Vascular Health and Risk Management, 13, 325–342. 10.2147/VHRM.S121661 [PubMed: 28860793]

Hughes S, Szeki I, Nash MJ, & Thachil J (2014). Anticoagulation in chronic kidney disease patients-the practical aspects. Clinical Kidney Journal, 7(5), 442–449. 10.1093/ckj/sfu080 [PubMed: 25878775]

Jin L, Pandey P, Babine RE, Weaver DT, Abdel-Meguid SS, & Strickler JE (2005). Mutation of surface residues to promote crystallization of activated factor XI as a complex with benzamidine: An essential step for the iterative structure-based design of factor XI inhibitors. Acta Crystallographica. Section D, Biological Crystallography, 61(Pt 10), 1418–1425. 10.1107/S0907444905024340 [PubMed: 16204896]

Jun M, Lix LM, Durand M, Dahl M, Paterson JM, Dormuth CR, Ernst P, Yao S, Renoux C, Tamim H, Wu C, Mahmud SM, Hemmelgarn BR, & Canadian Network for Observational Drug Effect Studies (CNODES) Investigators. (2017). Comparative safety of direct oral anticoagulants and warfarin in venous thromboembolism: Multicentre, population based, observational study. BMJ, 359, j4323. 10.1136/bmj.j4323 [PubMed: 29042362]

Kar S, Bankston P, Afosah DK, & Al-Horani RA (2021). Lignosulfonic acid sodium is a noncompetitive inhibitor of human factor XIa. Pharmaceuticals, 14(9), 886. 10.3390/ph14090886 [PubMed: 34577586]

Kar S, Mottamal M, & Al-Horani RA (2020). Discovery of benzyl tetraphosphonate derivative as inhibitor of human factor Xia. ChemistryOpen, 9(11), 1161–1172. 10.1002/open.202000277 [PubMed: 33204588]

Kassack MU, Braun K, Ganso M, Ullmann H, Nickel P, Böing B, Müller G, & Lambrecht G (2004). Structure-activity relationships of analogues of NF449 confirm NF449 as the most potent and selective known P2X1 receptor antagonist. European Journal of Medicinal Chemistry, 39(4), 345–357. 10.1016/j.ejmech.2004.01.007 [PubMed: 15072843]

Kimachi M, Furukawa TA, Kimachi K, Goto Y, Fukuma S, & Fukuhara S (2017). Direct oral anticoagulants versus warfarin for preventing stroke and systemic embolic events among atrial fibrillation patients with chronic kidney disease. The Cochrane Database of Systematic Reviews, 11(11), CD011373. 10.1002/14651858.CD011373.pub2 [PubMed: 29105079]

Kubitza D, Heckmann M, Distler J, Koechel A, Schwers S, & Kanefendt F (2022). Pharmacokinetics, pharmacodynamics and safety of BAY 2433334, a novel activated factor XI inhibitor, in healthy volunteers: A randomized phase 1 multiple-dose study. British Journal of Clinical Pharmacology. 10.1111/bcp.15230. Online ahead of print.

Larsen TB, Skjøth F, Nielsen PB, Kjældgaard JN, & Lip GY (2016). Comparative effectiveness and safety of non-vitamin K antagonist oral anticoagulants and warfarin in patients with atrial fibrillation: Propensity weighted nationwide cohort study. BMJ, 353, i3189. 10.1136/bmj.i3189 [PubMed: 27312796]

Lea T (2015). Caco-2 Cell Line. In Verhoeckx K, Cotter P, López-Expósito I, Kleiveland C, Lea T, Mackie A, Requena T, Swiatecka D & Wichers H (Eds.), The Impact of Food Bioactives on Health: In vitro and ex vivo models [Internet]. Cham: Springer.

Lin YC, Boone M, Meuris L, Lemmens I, Van Roy N, Soete A, Reumers J, Moisse M, Plaisance S, Drmanac R, Chen J, Speleman F, Lambrechts D, Van de Peer Y, Tavernier J, & Callewaert N (2014). Genome dynamics of the human embryonic kidney 293 lineage in response to cell biology manipulations. Nature Communications, 5, 4767. 10.1038/ncomms5767

Liu J, Pham PT, Skripnikova EV, Zheng S, Lovings LJ, Wang Y, Goyal N, Bellow SM, Mensah LM, Chatters AJ, Bratton MR, Wiese TE, Zhao M, Wang G, & Foroozesh M (2015). A ligand-based drug design. Discovery of 4-trifluor omethyl-7,8-pyranocoumarin as a selective inhibitor of human cytochrome P450 1A2. Journal of Medicinal Chemistry, 58(16), 6481–6493. 10.1021/acs.jmedchem.5b00494 [PubMed: 26222195]

Lutz J, Jurk K, & Schinzel H (2017). Direct oral anticoagulants in patients with chronic kidney disease: Patient selection and special considerations. International Journal of Nephrology and Renovascular Disease, 10, 135–143. 10.2147/IJNRD.S105771 [PubMed: 28652799]

McCain DF, Wu L, Nickel P, Kassack MU, Kreimeyer A, Gagliardi A, Collins DC, & Zhang ZY (2004). Suramin derivatives as inhibitors and activators of protein-tyrosine phosphatases. The Journal of Biological Chemistry, 279(15), 14713–14725. 10.1074/jbc.M312488200 [PubMed: 14734566]

McMullen BA, Fujikawa K, & Davie EW (1991). Location of the disulfide bonds in human coagulation factor XI: The presence of tandem apple domains. Biochemistry, 30(8), 2056–2060. 10.1021/bi00222a008 [PubMed: 1998667]

Meijers JC, Davie EW, & Chung DW (1992). Expression of human blood coagulation factor XI: Characterization of the defect in factor XI type III deficiency. Blood, 79(6), 1435–1440. [PubMed: 1547342]

Meijers JC, Tekelenburg WL, Bouma BN, Bertina RM, & Rosendaal FR (2000). High levels of coagulation factor XI as a risk factor for venous thrombosis. The New England Journal of Medicine, 342(10), 696–701. 10.1056/NEJM200003093421004 [PubMed: 10706899]

Mohammed BM, Matafonov A, Ivanov I, Sun MF, Cheng Q, Dickeson SK, Li C, Sun D, Verhamme IM, Emsley J, & Gailani D (2018). An update on factor XI structure and function. Thrombosis Research, 161, 94–105. 10.1016/j.thromres.2017.10.008 [PubMed: 29223926]

Perera V, Wang Z, Luettgen J, Li D, DeSouza M, Cerra M, & Seiffert D (2022). First-in-human study of milvexian, an oral, direct, small molecule factor XIa inhibitor. Clinical and Translational Science, 15(2), 330–342. 10.1111/cts.13148 [PubMed: 34558200]

Salomon O, Steinberg DM, Koren-Morag N, Tanne D, & Seligsohn U (2008). Reduced incidence of ischemic stroke in patients with severe factor XI deficiency. Blood, 111(8), 4113–4117. 10.1182/blood-2007-10-120139 [PubMed: 18268095]

Salomon O, Steinberg DM, Zucker M, Varon D, Zivelin A, & Seligsohn U (2011). Patients with severe factor XI deficiency have a reduced incidence of deep-vein thrombosis. Thrombosis and Haemostasis, 105(2), 269–273. 10.1160/TH10-05-0307 [PubMed: 21057700]

Schrödinger. (2017). Schrödinger release 2017–1: Glide. Schrödinger, LLC, New York, NY, USA. https://www.schrodinger.com/citations

Suri MF, Yamagishi K, Aleksic N, Hannan PJ, & Folsom AR (2010). Novel hemostatic factor levels and risk of ischemic stroke: The Atherosclerosis Risk in Communities (ARIC) Study. Cerebrovascular Diseases, 29(5), 497–502. 10.1159/000297966 [PubMed: 20299790]

Trapp J, Meier R, Hongwiset D, Kassack MU, Sippl W, & Jung M (2007). Structure-activity studies on suramin analogues as inhibitors of NAD+-dependent histone deacetylases (sirtuins). ChemMedChem, 2(10), 1419–1431. 10.1002/cmdc.200700003 [PubMed: 17628866]

Undas A, Slowik A, Gissel M, Mann KG, & Butenas S (2011). Circulating activated factor XI and active tissue factor as predictors of worse prognosis in patients following ischemic cerebrovascular events. Thrombosis Research, 128(5), e62–e66. 10.1016/j.thromres.2011.06.010 [PubMed: 21820158]

Undas A, Slowik A, Gissel M, Mann KG, & Butenas S (2012). Active tissue factor and activated factor XI in patients with acute ischemic cerebrovascular events. European Journal of Clinical Investigation, 42(2), 123–129. 10.1111/j.1365-2362.2011.02565.x [PubMed: 21707613]

Wang X, Smith PL, Hsu MY, Gailani D, Schumacher WA, Ogletree ML, & Seiffert DA (2006). Effects of factor XI deficiency on ferric chloride-induced vena cava thrombosis in mice. Journal of Thrombosis and Haemostasis, 4(9), 1982–1988. 10.1111/j.1538-7836.2006.02093.x [PubMed: 16961605]

Weitz JI, Strony J, Ageno W, Gailani D, Hylek EM, Lassen MR, Mahaffey KW, Notani RS, Roberts R, Segers A, Raskob GE, & AXIOMATIC-TKR Investigators. (2021). Milvexian for the prevention of venous thromboembolism. The New England Journal of Medicine, 385(23), 2161–2172. 10.1056/NEJMoa2113194 [PubMed: 34780683]

Wong PC, Crain EJ, Bozarth JM, Wu Y, Dilger AK, Wexler RR, Ewing WR, Gordon D, & Luettgen JM (2022). Milvexian, an orally bioavailable, small-molecule, reversible, direct inhibitor of factor XIa: In vitro studies and in vivo evaluation in experimental thrombosis in rabbits. Journal of Thrombosis and Haemostasis, 20(2), 399–408. 10.1111/jth.15588 [PubMed: 34752670]

Yan L, & Müller CE (2004). Preparation, properties, reactions, and adenosine receptor affinities of sulfophenylxanthine nitrophenyl esters: Toward the development of sulfonic acid prodrugs with peroral bioavailability. Journal of Medicinal Chemistry, 47(4), 1031–1043. [PubMed: 14761205]

Yang L, Sun MF, Gailani D, & Rezaie AR (2009). Characterization of a heparin-binding site on the catalytic domain of factor XIa: Mechanism of heparin acceleration of factor XIa inhibition by the serpins antithrombin and C1-inhibitor. Biochemistry, 48(7), 1517–1524. 10.1021/bi802298r [PubMed: 19178150]

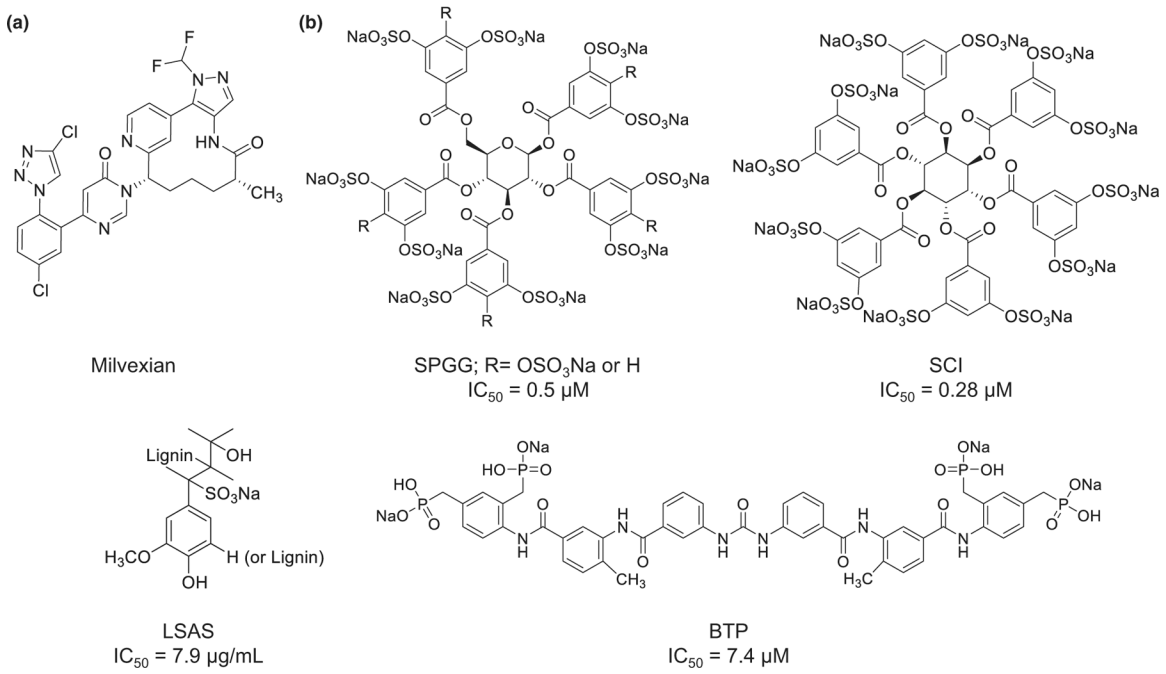

FIGURE 1.

(a) The chemical structure of active site inhibitor of human FXIa that is in advanced clinical trials. (b) The chemical structures of previously reported allosteric inhibitors of human FXIa

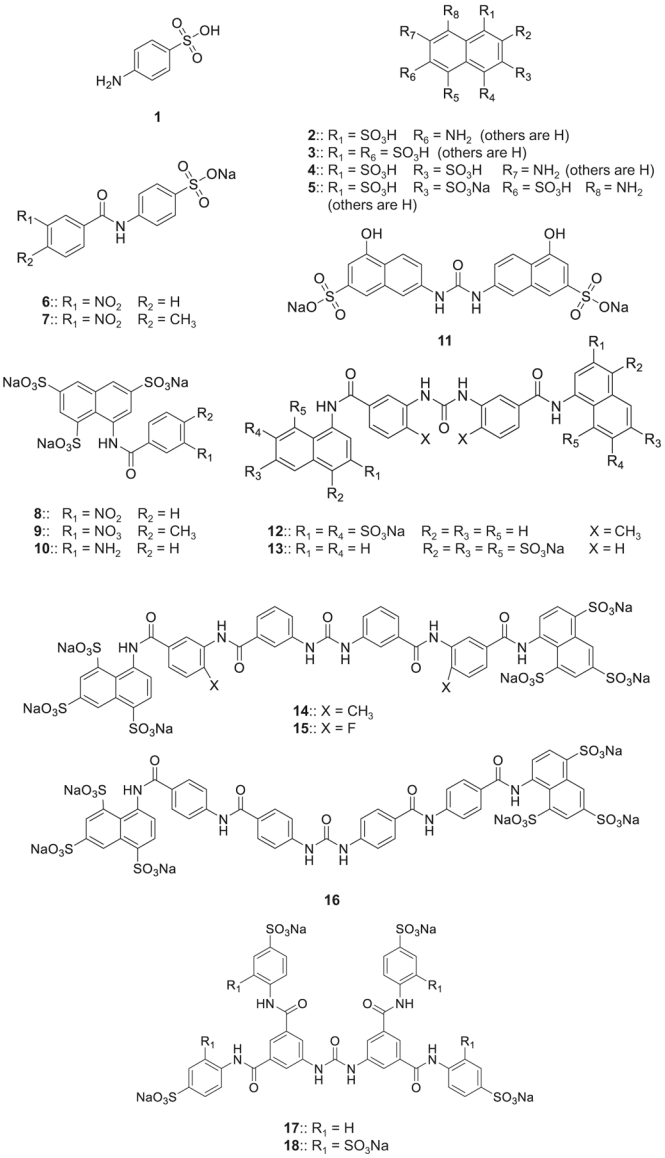

FIGURE 2.

Chemical structures of sulfonated molecules (**1**–**18**) that were investigated as inhibitors of human FXIa in this study

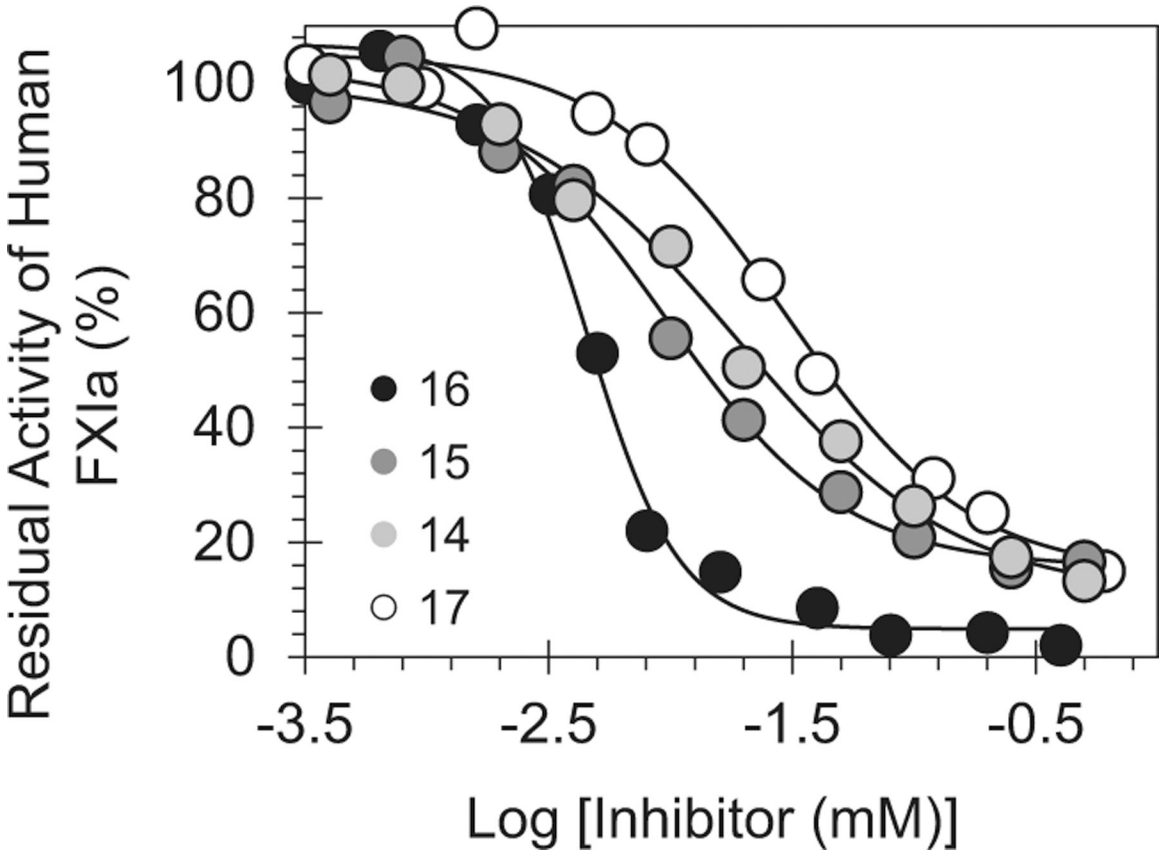

FIGURE 3.

Direct inhibition of FXIa by sulfonated molecules (**14**–**17**). The inhibition potential was investigated using S-2366 hydrolysis assay. The solid traces are the sigmoidal data fits using Equation 1 to obtain the values of IC_{50}, HS, and $\Delta Y\%$

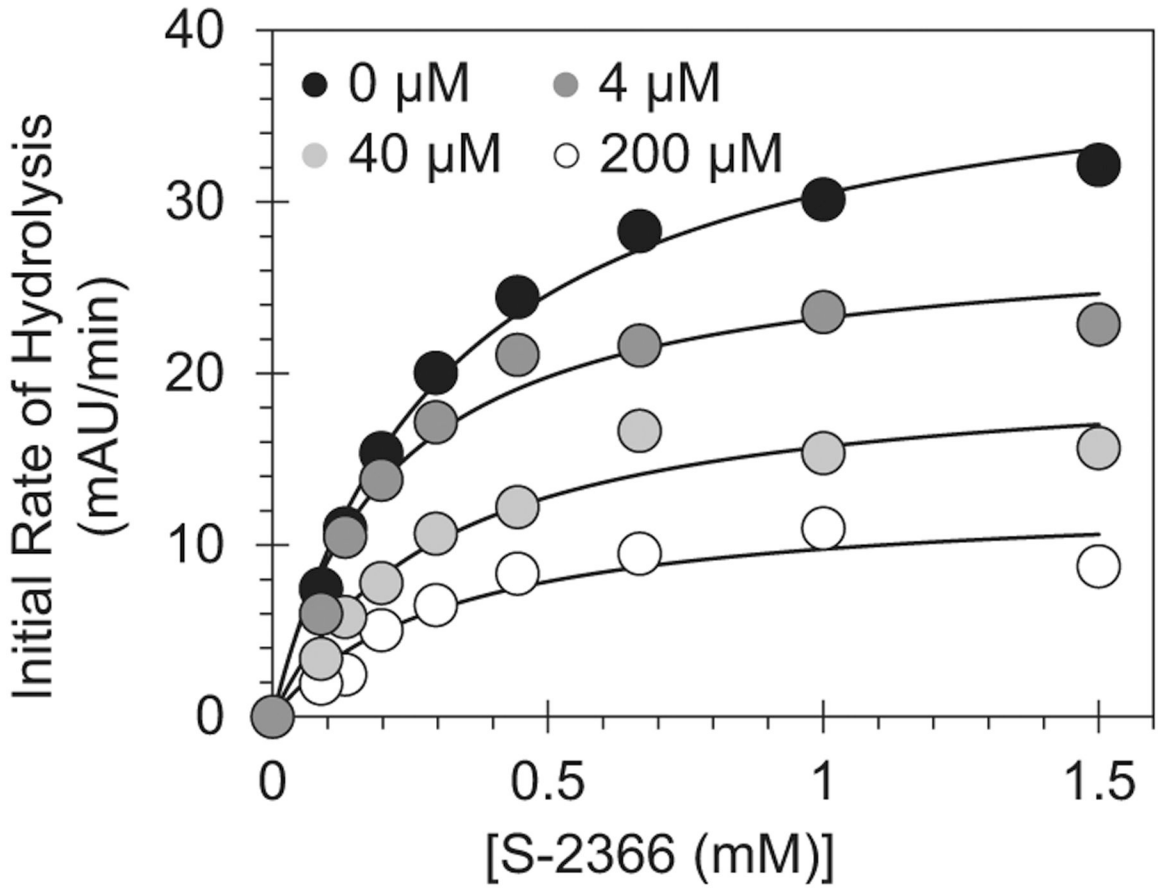

FIGURE 4.

Michaelis–Menten kinetics of FXIa-mediated hydrolysis of S-2366 in the presence of inhibitor **14**. The initial rate of hydrolysis at different concentrations of the substrate was measured using wild-type human FXIa in pH 7.4 buffer. [Inhibitor **14**] were 0 (●), 4 (●), 40 (●), 200 μM (○). The solid traces are the non-linear regressional fits to the data by Equation 2

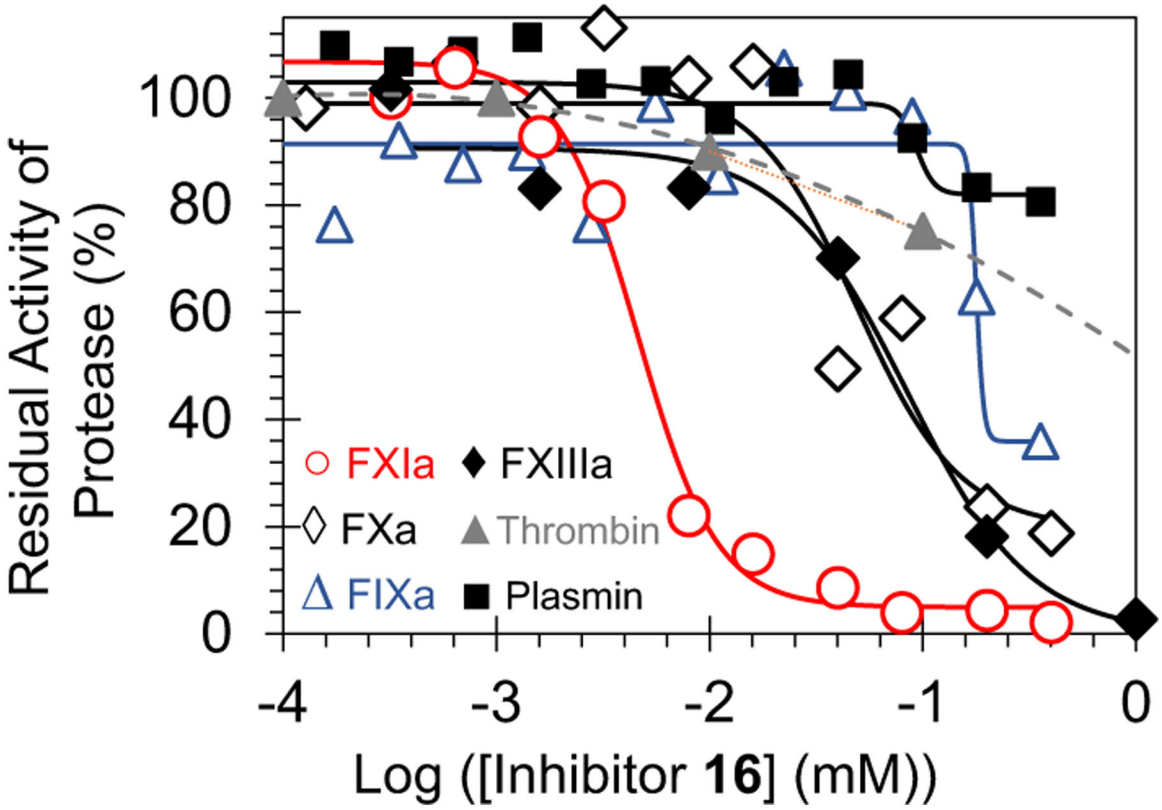

FIGURE 5.

Direct inhibition of multiple proteases by inhibitor **16**. Inhibition profiles of FXIa (○), FXIIIa (♦), FXa (◊), thrombin (▲), FIXa (Δ), and plasmin (■) are presented. The inhibition potential was studied using previously reported chromogenic substrate hydrolysis assays. The solid traces are the sigmoidal data fits using Equation 1 to obtain the values of IC_{50}, HS, and $\Delta Y\%$

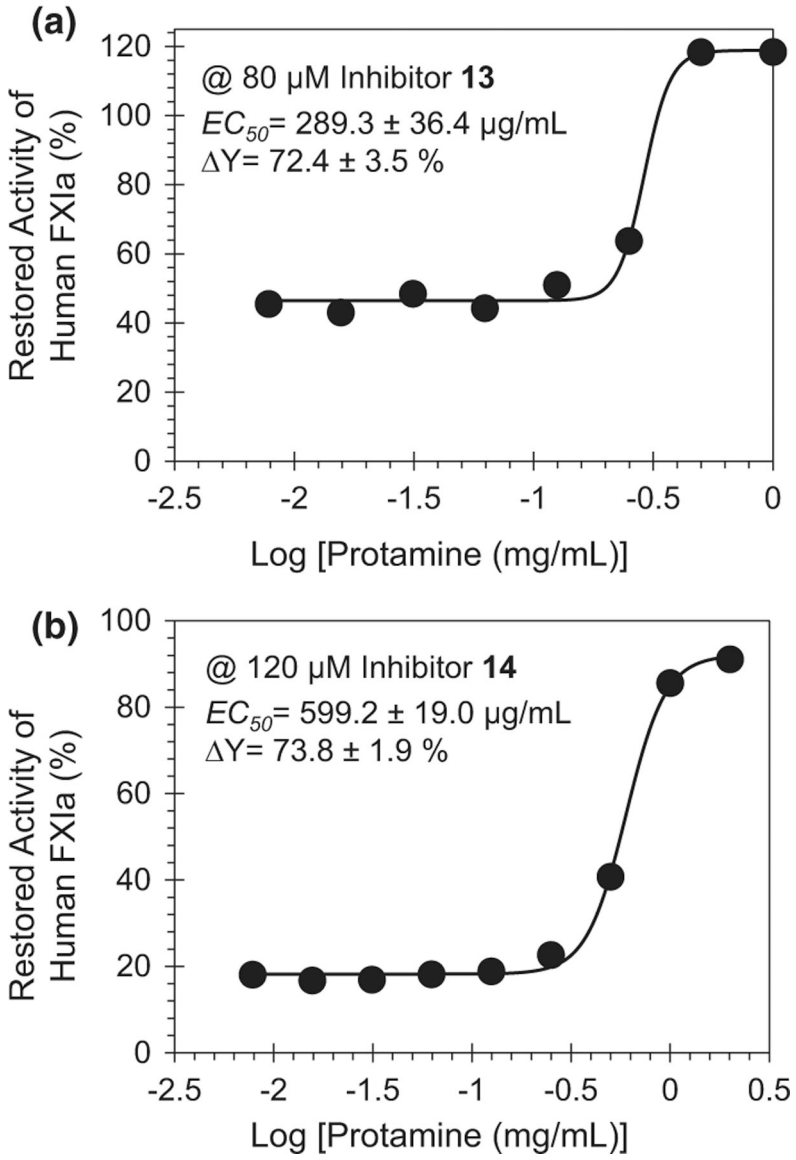

FIGURE 6.

Reversibility of sulfonated molecules' interaction with FXIa by protamine sulfate. Shown is the in vitro restored FXIa activity (%) inhibited by molecule **13** (80 μM) (a) or molecule **14** (120 μM) (b) in the presence of increasing concentration of protamine sulfate. The restored activity profiles were constructed spectrophotometrically at 37°C and pH 7.4. The solid traces are the data fits by equation 3 to obtain the EC_{50} as described in Materials and Methods

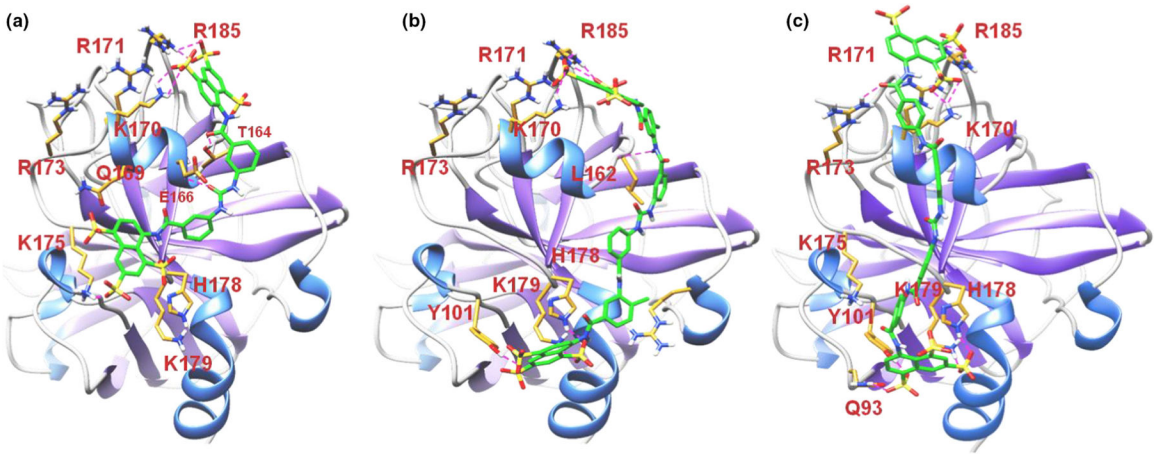

FIGURE 7.

Non-conserved anion-binding site in FXIa's catalytic domain is depicted as a putative binding site for inhibitors **13**, **15**, and **16**. In this molecular docking exercise, we attempted to identify potential interactions with Arg/Lys residues that are involved in heparin and polyphosphate recognition of FXI(a) during its inhibition and activation, respectively

TABLE 1

Human FXIa inhibition by sulfonated molecules (**1–18**)[a]

Inhibitors	IC_{50} (μM)	HS	Δ*Y* (%)
1–10	>50[b]	*NA*[c]	*NA*
11	24.5 ± 2.5[d]	1.5 ± 0.2	98.6 ± 4.2
12	>500	*NA*	*NA*
13	25.9 ± 4.9	0.7 ± 0.1	90.4 ± 6.1
14	18.7 ± 2.9	0.9 ± 0.1	89.6 ± 5.2
15	9.5 ± 1.0	1.2 ± 0.2	87.3 ± 3.4
16	4.6 ± 0.4	2.3 ± 0.4	101.8 ± 4.0
17	29.5 ± 4.6	1.2 ± 0.2	90.9 ± 5.8
18	>500	*NA*	*NA*
BTP	7.4 ± 0.9[e]	1.9 ± 0.5	68.0 ± 3.7

[a]The IC_{50}, HS, and ΔY were obtained via the non-linear regression analysis of FXIa direct inhibition in Tris–HCl buffer. Inhibition was followed by the spectrophotometric measurement of residual FXIa activity.

[b]Estimated measurement based on the highest concentration used in the study.

[c]Not available.

[d]Errors represent ±1 S.E.

[e]From reference (Kar et al., 2020).

TABLE 2

Michaelis–Menten kinetics of FXIa-mediated hydrolysis of S-2366 in the presence of inhibitors **14**[a]

[14] (μM)	S-2366 K_M (mM)	V_{MAX}(mAU/min)
0	0.31 ± 0.03[b]	40.0 ± 1.3
4	0.21 ± 0.04	28.1 ± 1.5
40	0.30 ± 0.07	20.4 ± 1.7
200	0.32 ± 0.11	12.9 ± 1.6

[a] K_M and V_{MAX} values of S-2366 hydrolysis by FXIa were measured as detailed in Materials and Methods. mAU depicts milliabsorbance units.

[b] Error represents ±1 S.E.

TABLE 3

Inhibition of thrombin and FXa by sulfonated molecules (11–18)[a]

	Thrombin			FXa		
Inhibitors	**IC_{50} (μM)**	**HS**	**ΔY (%)**	**IC_{50} (μM)**	**HS**	**ΔY (%)**
11	>100[b]	*NA*[c]	*NA*	>100	*NA*	*NA*
13	>500	*NA*	*NA*	86.2 ± 9.1[d]	4.9 ± 2.5	52.9 ± 4.2
14	16.6 ± 3.7	2.0 ± 0.9	52.9 ± 5.2	19.9 ± 4.5	1.7 ± 0.7	76.5 ± 7.8
15	19.0 ± 4.5	1.6 ± 0.6	40.0 ± 3.9	181.6 ± 148.2	0.7 ± 0.4	99.0 ± 51.6
16	>100	*NA*	*NA*	48.6 ± 14.8	1.8 ± 1.0	83.3 ± 15.0
17	>100	*NA*	*NA*	>100	*NA*	*NA*

[a] IC_{50}, HS, and ΔY were obtained via non-linear regression analysis of inhibition of human FIIa and FXa in appropriate Tris–HCl buffer. Inhibition was followed by the spectrophotometric measurement of residual FIIa or FXa activity.

[b] Estimated value based on the highest concentration used in the study.

[c] Not available.

[d] Errors represent ±1 S.E.

TABLE 4

Inhibition of coagulation proteins by molecules **13**, **14**, and **16**[a]

Inhibitor	Inhibition parameters	Factor XIa	Thrombin	Factor Xa	Factor IXa	Factor XIIIa
13	IC_{50} (μM)	25.9 ± 4.9[b]	>500	>500	*ND*	161.6 ± 37.1
	HS	0.7 ± 0.1	*ND*[c]	*ND*	*ND*	0.9 ± 0.2
	Δ*Y* (%)	90.4 ± 6.1	*ND*	*ND*	*ND*	83.5 ± 16.1
14	IC_{50} (μM)	18.7 ± 2.9	16.6 ± 3.7	19.9 ± 4.5	*ND*	85.2 ± 12.6
	HS	0.9 ± 0.1	2.0 ± 0.9	1.7 ± 0.7	*ND*	1.3 ± 0.2
	Δ*Y* (%)	89.6 ± 5.2	52.9 ± 5.2	76.5 ± 7.8	*ND*	89.6 ± 5.1
16	IC_{50} (μm)	4.6 ± 0.4	>100	48.6 ± 14.8	>350	83.9 ± 27.6
	HS	2.3 ± 0.4	*ND*	1.8 ± 1.0	*ND*	1.5 ± 0.8
	Δ*Y* (%)	101.8 ± 4.0	*ND*	83.3 ± 15.0	*ND*	90.7 ± 15.2

[a] IC_{50}, HS, and Δ*Y* were obtained via non-linear regression analysis of direct inhibition of human enzymes in appropriate buffers.

[b] Errors represent ±1 S.E.

[c] Not determined.

TABLE 5

Inhibition of inflammatory, fibrinolysis, and digestive proteases by molecules **13**, **14**, and **16**[a]

Inhibitor	Inhibition parameters	Neutrophil Elastase	Cathepsin G	Proteinase 3	Plasmin	Trypsin	Chymotrypsin
13	IC_{50} (μm)	33.4 ± 9.9[b]	*ND*[c]	*ND*	>500	>150	>150
	HS	1.2 ± 0.5	*ND*	*ND*	*ND*	*ND*	*ND*
	Δ*Y*(%)	62.7 ± 6.9	*ND*	*ND*	*ND*	*ND*	*ND*
14	IC_{50} (μM)	13.4 ± 1.1	*ND*	*ND*	40.1 ± 12.5	>150	>150
	HS	1.8 ± 0.3	*ND*	*ND*	0.9 ± 0.3	*ND*	*ND*
	Δ*Y*(%)	86.3 ± 2.9	*ND*	*ND*	91.4 ± 11.1	*ND*	*ND*
16	IC_{50} (μm)	0.22 ± 0.00	0.57 ± 0.05	34.2 ± 12.7	>180	>180	>180
	HS	2.6 ± 0.1	1.8 ± 0.3	0.8 ± 0.2	*ND*	*ND*	*ND*
	Δ*Y*(%)	105.4 ± 1.0	89.7 ± 2.9	49.2 ± 8.0	*ND*	*ND*	*ND*

[a] IC_{50}, HS, and ΔY were obtained via non-linear regression analysis of direct inhibition of human enzymes in appropriate buffers.

[b] Errors represent ±1 S.E.

[c] Not determined.

TABLE 6

Effects of sulfonated molecules on the clotting times of human plasma[a]

Inhibitors	$APTT_{1.5x}$ (μM)	$PT_{1.5x}$ (μM)
13	392.9 ± 19.6[b]	481.4 ± 24.1
14	337.7 ± 16.9	446.7 ± 22.3
15	307.6 ± 15.4	402.3 ± 20.1
16	354.3 ± 17.7	419.5 ± 21.0
17	459.1 ± 23.0	511 ± 25.6

[a]Presented are the concentrations of each sulfonated molecule that are required to prolong the APTT or the PT of normal human plasma by 1.5-fold.

[b]Estimated errors of ~1 S.E.